94. Maeda H, Matsumura Y, Oda T, Sasamoto K (1986) Cancer selective macromolecular therapeusis; tailoring of an antitumor protein drug. *In*: Feeney RE, Whitaker JR (eds): Protein tailoring for food and medical uses. Marcel Dekker, New York

95. Davis S, Abuchowski A, Park YK, Davis FF (1981) Alteration of the circulating life and antigenic properties of bovine adenosine deaminase in mice by attachment of polyethylene glycol. Clin Exp Immunol 46:649-652

96. Ensor CM, Holtsberg FW, Bomalaski JS, Clark MA (2002) Pegylated arginine deiminase (ADI-SS PEG20,000 mw) inhibits human melanomas and hepatocellular carcinomas in vitro and in vivo. Cancer Res 62:5443-5450

97. Zhao W, Zhuang S Qi XR (2011) Comparative study of the in vitro and in vivo characteristics of cationic and neutral liposomes. Int J Nanomed 6:3087-3098

98. Maeda H, Kimura I, Sasaki Y et al (1992) Toxicity of bilirubin and detoxification by PEG-bilirubin oxidase conjugate: A new tactic for treatment of jaundice. *In*: J. M. Harris (ed): Poly(Ethylene Glycol) Chemistry: Biotech Biomed Applications, Plenum Press, New York, p. 153-169

99. Kimura M, Matsumura Y, Miyauchi Y and Maeda H (1988) A new tactic for the treatment of jaundice: An injectable polymer-conjugated bilirubin oxidase. Proc Soc Exp Biol Med 188: 364-369

100. Li CY, Shan S, Huang Q etal (2000) Initial Stage of Tumor Cell-Induced Angiogenesis: Evaluation Via Skin Window Chambers in Rodent Models. J Natl Cancer Inst 92: 143-147

Figure 1

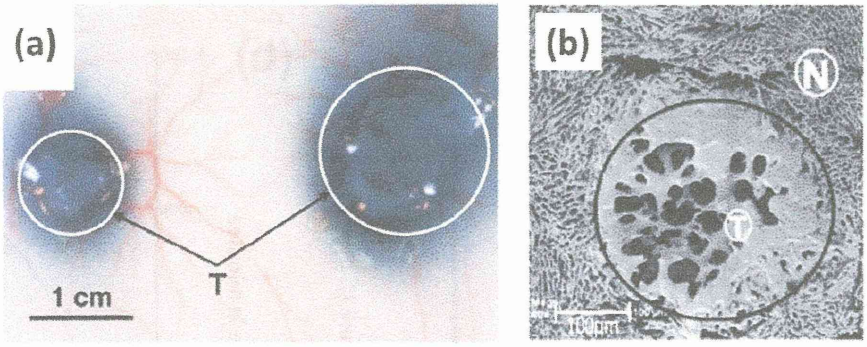

Fig. 1. Illustration of the EPR effect. (a) Tumor-selective accumulation of the putative macromolecular drug Evans blue-albumin complex (MW 67 kDa). The blue color in the macroscopic image indicates macromolecular drug delivery to S-180 tumor implanted in the skin of mice at 24 h after i.v. injection of Evans blue (10 mg/kg). The tumor sites (T, circles, and arrows) show progressive accumulation of Evans blue-albumin, in both small and large tumor. (b) Scanning electron microscopic image of metastatic liver cancer. The tumor (T, circle) is a micrometastatic tumor nodule; even this small nodule shows leakage of a polymer (polyarylate), which is not seen in the surrounding normal tissue (N, in the liver). (Adapted from refs [23]). Dewhirst et al showed that tumor angiogenesis becomes visible when 100-300 tumor cells present [100].

Figure 2.

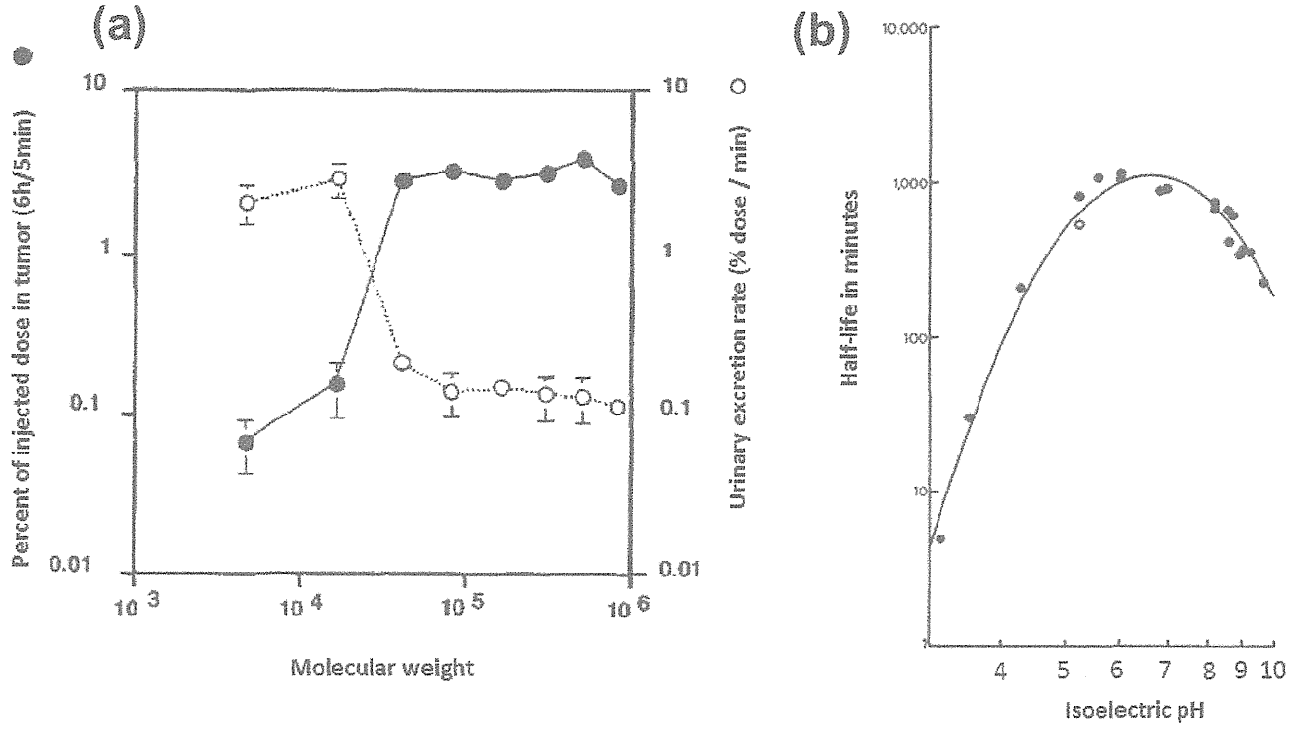

Fig. 2. Influence of the size and charge of macromolecules on their distribution in tumors and plasma concentration. (a) HPMA copolymers, labeled with ^{125}I and of different sizes, were injected i.v. into tumor-bearing mice. The percentage of the injected dose of HPMA in tumor and in urine was calculated. (Adapted from ref [16,23,24]). (b) L-Asparaginase derivatives (MW 120 kDa) with different isoelectric points (pI) after chemical modification were injected i.v. into rabbits (2500 IU/kg), after which the remaining activity of each L-asparaginase derivative was measured and their half-life values in systemic circulation were calculated. (Adapted from ref [39])

Figure 3

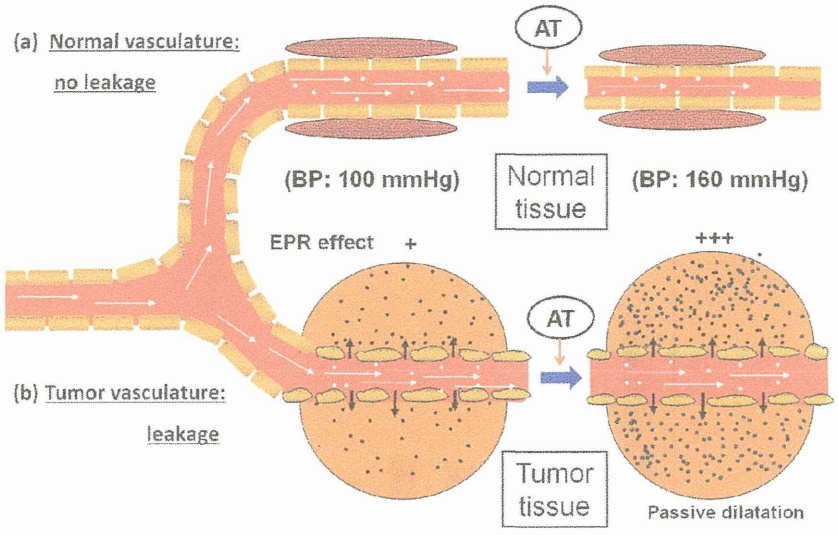

Fig. 3. Diagrammatic representation of the EPR effect and the effect of AT-II-induced enhancement of macromolecular drug delivery to normal and tumor tissue. In the lower part (tumor tissue), angiotensin II (AT-II) infusion induced high blood pressure (e.g., 100 mmHg → 160 mmHg), which caused endothelial cell-cell junctions in the tumor to open and blood flow to increase, with leakage of the macromolecular drug (dark dots). In contrast, normal blood vessels (upper part) constricts in response to AT-II, and tighten the endothelial cell-cell junctions that cause high blood pressure, with no leakage of the drug. AT-II-induced hypertension thus resulted in greater (2–3 fold) leakage of drug into the tumor without increased drug accumulation into normal tissue. (Adapted from ref [24])

Figure 4

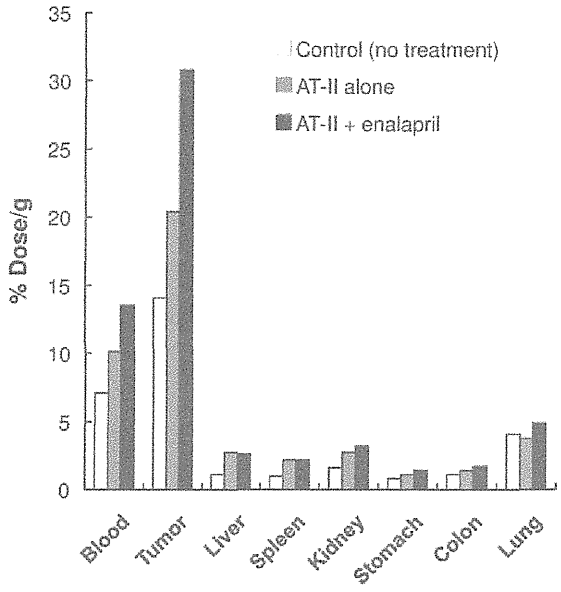

Fig. 4. Augmentation of the EPR effect and delivery of monoclonal antibody to the tumor by using AT-II and the ACE inhibitor enalapril. Human SW1116 colon cancer-bearing nude mice were injected i.v. with ^{125}I-labeled monoclonal antibody A7 with or without AT-II and enalapril. (Adapted from ref [57])

Figure 5

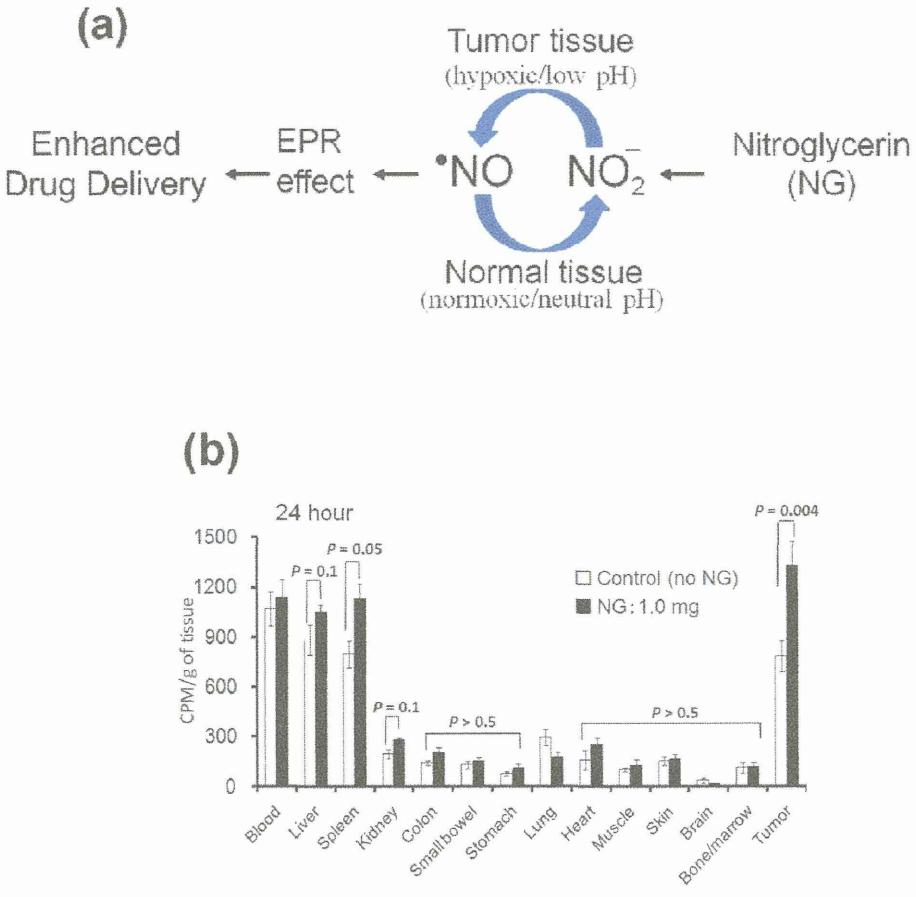

Fig. 5. Nitroglycerin (NG)-induced increase in accumulation of polymer-conjugated drug in tumors. (a) Mechanism of selective NO generation in tumor. NO was generated from nitrite, predominantly in hypoxic tumor tissue, not in normal tissue. (b) In vivo evaluation of the potentiation of drug delivery to tumor by nitroglycerin that was applied as an ointment to anywhere on the skin of S-180 tumor-bearing mice at a dose of 1.0 mg/mouse. Pegylated-^{65}Zn-labeled Zn-protoporphyrin was then injected i.v. into the tumor-bearing mice. After 24 h, anesthetized mice were dissected and radioactivity of each tissue was counted. (Adapted from refs [23,69])

Figure 6

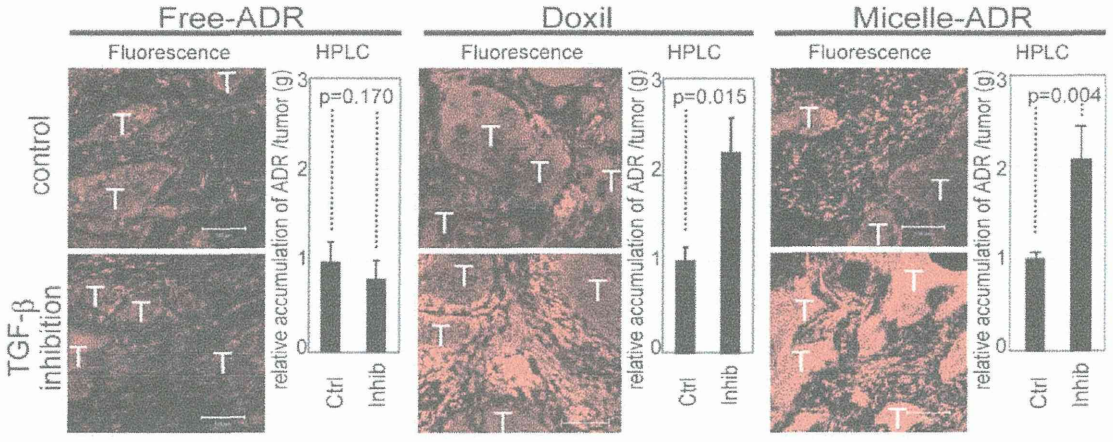

Fig. 6. Biodistribution of free ADR, Doxil, and ADR-micelles in the pancreatic cancer BxPC3 model in mice. Distributions of free ADR, Doxil, and ADR-micelles (each at 8 mg/kg) with or without TGF-β receptor inhibitor (LY364947) (1 mg/kg) were evaluated via fluorescent microscopy at 24 h after drug administration. Bar graphs at the right show relative quantitative results for the accumulation of drugs in tumors obtained by high-performance liquid chromatography (HPLC). Treatment with TGF-β receptor inhibitor resulted in about a two-fold enhancement of accumulation of Doxil and ADR micelles. Error bars in the graphs represent standard errors; *P* values were calculated by using Student's *t* test. T, nests of tumor cells in tumor tissues; Doxil, pegylated liposome; Ctrl, control without the inhibitor; Inhib, inhibitor. See text for detail. (Adapted from ref [87])

Figure 7

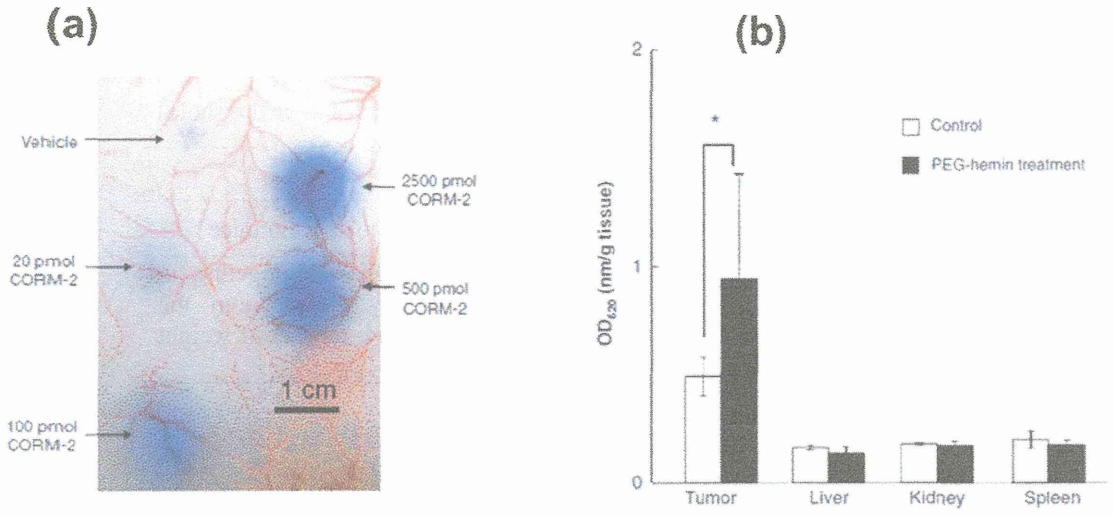

Fig. 7. CO-enhanced accumulation of Evans blue-albumin complex in tumors. (a) Different concentrations of the CO-releasing agent CORM-2 were administered subcutaneously, followed by i.v. injection of Evans blue (10 mg/kg). The dye-albumin complex was allowed to extravasate for 2 h. (b) At 24 h after the i.v. injection of an HO-1 inducer, pegylated hemin (10 mg/kg hemin equivalent), Evans blue was injected as in (a). After another 24 h, mice were killed and dissected to obtain the tissues. Control mice were not treated with pegylated hemin. The blue dye complexed with albumin in each tissue was extracted with formamide, and the degree of extravasation was quantified by means of absorbance at 620 nm. (Adapted from ref [25])

Table 1. Characteristics of the EPR effect of nanomedicine or macromolecular drugs

Biocompatibility	No interaction with blood components or blood vessels, no antigenicity, no clearance by the reticuloendothelial system, no cell lysis
Molecular size	Greater than 40 kDa (larger than the renal clearance threshold)
Surface charge	Weakly negative to near neutral
Time required to achieve	Longer than several hours in systemic circulation in mice
Drug retention time	Mostly days to weeks, in great contrast to passive targeting (in which low-MW molecules are rapidly cleared into the systemic circulation in a few min. cf. low molecular weight contrast agent (see text).

Table 2. Plasma clearance times of selected modified and native proteins in vivo

Protein	Species difference, original/test animal	Probe modification	pI[a]	MW (kDa)	$t_{1/2}$[b]	Note	Ref
• **Albumin**	Mouse/mouse	None	4.8	68	72–96 h	Native, syngeneic	[20,94]
Albumin	Mouse/mouse	DTPA (^{51}Cr)[d]	≦4.8	-	6 h	Slightly surface modified, loss of amino group, syngeneic	
Albumin	Cow/mouse	DTPA (^{51}Cr)[d]	≦4.8	-	1 h	Slightly surface modified, loss of amino group, xenogeneic	
Formaldehyde modified albumin	Human/rat	Formaldehyde ^{125}I	≦4.8	-	25 min	Denatured, loss of amino group, xenogeneic	
• **α_2-Macroglobulin**	Human/mouse	^{125}I	5.3	180×4	140 h	Native, xenogeneic	[20,94]
α_2-Macroglobulin-plasmin complex	Human/mouse	^{125}I	-	180×4	5 min	Inhibitor-protein complex, xenogeneic	
• **Immunoglobulin (IgG)**	Mouse/mouse	DTPA[d]	≦6.8	159	60 h	Slightly surface modified, loss of amino group, syngeneic	[20,94]
• **Interferon α**	Human/human	None		18	8 h (sc)[e]	$t_{1/2}$ 4 min	[20]
Pegylated interferon α2a	Human/human	PEG		52	80 h (sc)[e]		
• **Adenosine deaminase (ADA)**	Cow/mouse	None	4.9	38	<0.5 h	Native, xenogeneic	[95]
Pegylated ADA	Bovine/mouse	PEG[d]	-	>38	28 h, 3–6 days in humans	60% of primary amine conjugated with PEG (5000 Da), xenogeneic	
• **Arginine deiminase (ADI)**	*Mycoplasma hominis*/mouse	Native	5.5	46	<5 h	Native, xenogeneic	[96]
Pegylated ADI	*M. hominis*/mouse	PEG[d]	-	>46	~7 days	10–12 PEG (20,000 Da) attached to each ADI, xenogeneic	
• **Bilirubin oxidase, native[d]**	Microbial/mouse			52	0.25 h		[98,99]
Bilirubin oxidase PEG conjugate	Microbial/mouse			110	5 h		
• **D-amino acid oxidase native**	Pig/mouse			39	14 h		[41]
D-amino acid oxidase PEG conjugate	Pig/mouse			63	36 h		
• **Neocarzinostatin (NCS)**	*Streptomyces*/mouse	DTPA (^{51}Cr)[d]	3.4	12	1.8 min	Slightly surface modified, loss of amino group, xenogeneic	[20,94]
SMA-conjugated NCS (SMANCS)	*Streptomyces*/mouse	DTPA(^{51}Cr)[d], SMA	>3.0	17	19 min	Two chains of SMA (1200 Da) attached to each amino group of NCS; SMA is polyanionic, xenogeneic	

[a]Isoelectric point.
[b]Half-life in systemic circulation (minutes, hours, or days), given i.v. unless otherwise stated.
[c]From microbe, *Myrothecium verrucaria*
[d]DTPA or PEG was reacted with the primary amino group of a lysine residue or N-terminal residue, which made the group much less cationic.
[e]Subcutaneous.